Inflammation Research (2023) 72:1485–1500
https://doi.org/10.1007/s00011-023-01757-5

Inflammation Research

ORIGINAL RESEARCH PAPER

A positive feedback cycle between the alarmin S100A8/A9 and NLRP3 inflammasome-GSDMD signalling reinforces the innate immune response in *Candida albicans* keratitis

Xiaolong Fang[1,2,3] · Huifang Lian[2,3,4] · Shuang Liu[3,5] · Jingcun Dong[3,5] · Xia Hua[6] · Wenguang Li[7] · Chunyang Liao[3,5] · Xiaoyong Yuan[1,2]

Received: 23 April 2023 / Revised: 26 May 2023 / Accepted: 7 June 2023 / Published online: 19 June 2023
© The Author(s), under exclusive licence to Springer Nature Switzerland AG 2023

Abstract

Objective Fungal keratitis is a severe sight-threatening ocular infection, without effective treatment strategies available now. Calprotectin S100A8/A9 has recently attracted great attention as a critical alarmin modulating the innate immune response against microbial challenges. However, the unique role of S100A8/A9 in fungal keratitis is poorly understood.

Methods Experimental fungal keratitis was established in wild-type and gene knockout ($TLR4^{-/-}$ and $GSDMD^{-/-}$) mice by infecting mouse corneas with *Candida albicans*. The degree of mouse cornea injuries was evaluated by clinical scoring. To interrogate the molecular mechanism in vitro, macrophage RAW264.7 cell line was challenged with *Candida albicans* or recombinant S100A8/A9 protein. Label-free quantitative proteomics, quantitative real-time PCR, Western blotting, and immunohistochemistry were conducted in this research.

Results Herein, we characterized the proteome of mouse corneas infected with *Candida albicans* and found that S100A8/A9 was robustly expressed at the early stage of the disease. S100A8/A9 significantly enhanced disease progression by promoting NLRP3 inflammasome activation and Caspase-1 maturation, accompanied by increased accumulation of macrophages in infected corneas. In response to *Candida albicans* infection, toll-like receptor 4 (TLR4) sensed extracellular S100A8/A9 and acted as a bridge between S100A8/A9 and NLRP3 inflammasome activation in mouse corneas. Furthermore, the deletion of TLR4 resulted in noticeable improvement in fungal keratitis. Remarkably, NLRP3/GSDMD-mediated macrophage pyroptosis in turn facilitates S100A8/A9 secretion during *Candida albicans* keratitis, thus forming a positive feedback cycle that amplifies the proinflammatory response in corneas.

Conclusions The present study is the first to reveal the critical roles of the alarmin S100A8/A9 in the immunopathology of *Candida albicans* keratitis, highlighting a promising approach for therapeutic intervention in the future.

Keywords *Candida albicans* keratitis · Innate immunity · Alarmin S100A8/A9 · TLR4 pathway · NLRP3 inflammasome activation · Macrophage pyroptosis

Responsible Editor: John Di Battista.

✉ Chunyang Liao
cyliao@rcees.ac.cn

✉ Xiaoyong Yuan
yuanxy_cn@hotmail.com

[1] School of Medicine, Nankai University, Tianjin, China

[2] Tianjin Key Laboratory of Ophthalmology and Visual Science, Tianjin Eye Hospital, Tianjin Eye Institute, Tianjin, China

[3] State Key Laboratory of Environmental Chemistry and Ecotoxicology, Research Centre for Eco-Environmental Sciences, Chinese Academy of Sciences, Beijing, China

[4] Department of Ophthalmology, Baoding First Central Hospital, Baoding, Hebei, China

[5] University of Chinese Academy of Sciences, Beijing, China

[6] Aier Eye Hospital, Tianjin, China

[7] Institute of Genetics and Developmental Biology, Chinese Academy of Sciences, Beijing, China

Background

Fungal keratitis (FK) is a severe pathogenic condition that may lead to permanent visual impairment. FK seriously affects the quality of life of patients and has replaced bacterial keratitis in some regions as the major contributor to corneal blindness [1]. As a common keratomycosis, *Candida albicans* (*C. albicans*) keratitis often occurs secondary to preexisting ocular surface disease (dry eye, incomplete eyelid closure, viral keratitis, etc.) or compromised immunity (diabetes, immunosuppression, etc.) [2, 3], requiring a deep understanding of the molecular pathogenesis. The innate immune system constitutes the first line of defence against invading fungal pathogens, which detects distinct pathogen-associated molecular patterns (PAMPs) or damage-associated molecular patterns (DAMPs) (also known as alarmins) via pattern recognition receptors (PRRs) and is indispensable for maintaining corneal homeostasis [4–6]. Among the innate immune cells combating fungal infection, macrophages are considered one of the key cell types that can be activated by alarmins generated by damaged and dying cells [7, 8]. Upon interaction with PRRs, alarmins relay intracellular defence signals that culminate in the induction of inflammatory cytokines and chemokines to eliminate fungal pathogens [9].

S100A8 and S100A9 are S100 calcium-binding proteins and exert mainly biological functions by forming heterodimers (S100A8/A9 complex) after release from myeloid cells or epithelial cells [10]. The S100A8/A9 complex has attracted increasing interest as a vital alarmin modulating the inflammatory response under infection or sterile conditions. Extracellular S100A8/A9 interacts with cell surface recognition molecules, including toll-like receptor 4 (TLR4) and receptor of advanced glycation end products (RAGE), mediating multiple immune signalling pathways involved in NF-κB, MyD88, and p38/MAPK [11, 12]. While S100A8/A9 is important for tissue repair and regeneration [13], its deleterious role in accelerating the progression of numerous diseases has also been demonstrated. Emerging studies have described that S100A8/A9 is widely implicated in the pathogenesis of tumour development [14], systemic infections [15], acute coronary syndrome [16], and autoimmune diseases [17]. For example, severe acute respiratory syndrome coronavirus 2 (SARS-CoV-2) induced aberrant expression of S100A8/A9 in COVID-19 animal models, which subsequently resulted in immunological imbalance and the expansion of abnormal immature neutrophils in circulation [18]. Additionally, S100A8/A9 promoted corneal injuries by enhancing inflammatory responses in *Pseudomonas aeruginosa* keratitis [19]. Nevertheless, the correlation between S100A8/A9 and the progression of *C. albicans* keratitis is not fully understood. In addition, it is worth noting that S100A8/A9 has the ability to shape the phenotype and function of macrophages [20]. Thus, the effect of S100A8/A9 on macrophages during *C. albicans* keratitis warrants further research.

Inflammasomes are a group of multiprotein complexes in the cytoplasm, and the assembly of each inflammasome is determined by a unique sensor following the detection of PAMPs or other endogenous DAMPs, which facilitates Caspase-1 (CASP1) activation and the secretion of the cytokines IL-1β/IL-18 [21, 22]. Among the identified inflammasomes, NLRP3 inflammasome is considered to be the best understood in terms of molecular mechanisms in response to *C. albicans* infection, showing that candidalysin not only activated NLRP3 inflammasome-dependent CASP1 but also drove the inflammasome-independent cytolysis of macrophages [23]. Notably, several alarmins have been reported to contribute to the activation of inflammasomes, particularly NLRP3. Neutrophil-derived S100A8/A9 primed the NLRP3 inflammasome in acute myocardial infarction [24, 25], and HMGB1 was necessary for hepatocyte NLRP3 inflammasome activation in liver injury following heatstroke [26]. Our previous study demonstrated that the NLRP3 inflammasome-mediated gasdermin-D (GSDMD) pathway participated in the pathogenesis of *C. albicans* keratitis [27]. However, whether and how NLRP3 senses the alarmin S100A8/A9 in *C. albicans* keratitis and connects this endogenous danger signal to inflammatory and innate immune responses remain unknown.

Pyroptosis represents a form of regulated cell death seen primarily in inflammatory cells, such as macrophages, and may be triggered by bacterial or other pathogen infections [28]. This type of cell death is characterized by the requirement for the cleavage of GSDMD mediated by inflammatory caspases [29]. A strong relationship between pyroptosis and alarmins has been reported: it has been reported that immunostimulatory alarmins released during pyroptosis, including ATP and HMGB1, in turn enhance the pyroptosis of tumour cells and infiltrating immune cells, creating a positive feedback loop [30]. Moreover, the activation of the NLRP3 inflammasome causes not only the maturation of IL-1β and IL-18 but also the release of alarmins, such as HMGB1 [31, 32]. In our previous study, we found that GSDMD maturation is dependent on NLRP3 inflammasome activation in mouse corneas infected with *C. albicans* [27]. However, it is unclear whether NLRP3-mediated pyroptosis affects the release of the alarmin S100A8/A9.

To date, few studies on S100A8/A9 and *C. albicans* keratitis have been conducted, and the extracellular function of S100A8/A9 in fungal keratitis (FK) is unclear. In the current study, we identified S100A8/A9 as an alarmin molecule with a critical role in keratitis induced by *C. albicans*

using quantitative proteomics analysis. This study provides direct evidence that S100A8/A9 worsens corneal injuries by promoting TLR4-dependent NLRP3 inflammasome activation in macrophages following *C. albicans* infection. Interestingly, NLRP3-mediated macrophage pyroptosis in turn drives the production of S100A8/A9, which amplifies inflammatory signals and forms a regulatory circuit in the development of *C. albicans* keratitis. These results uncover the potential of therapeutically targeting alarmin S100A8/A9 for suppressing the excessive inflammatory response in fungal keratitis (FK) and provide information on the interaction between alarmins and inflammasome activation.

Methods

Establishing experimental fungal keratitis in a mouse model

Candida albicans strain SC5314 was purchased from the China General Microbiological Culture Collection Center (CGMCC, Beijing, China), and it was cultured on malt agar medium (BINDER, Qingdao, China) for three days at 25 °C. Colonies were collected and diluted in sterile PBS (phosphate-buffered saline) to yield a 2×10^5 CFU/μL inoculum based on an optical density (OD) at 600 nm with a conversion factor of 1 $OD_{600}=3\times10^7$ CFU/mL. Female C57BL/6 J mice aged 6–8 weeks were anaesthetized intraperitoneally (ip) with ketamine–xylazine (80 mg/kg), and then corneas were superficially scarified by a 22-gauge needle to make a grid-like scratch wound of 30 marks, followed by inoculation with 1×10^6 CFU of *C. albicans* to induce keratitis.

Quantitative proteomics analysis based on LC−MS/MS

Our main strategy for quantitative proteomics analysis was a label-free approach using an UltiMate 3000 nano UPLC system (Thermo Fisher Scientific, San Jose, CA, USA) and a Thermo Fisher Orbitrap mass spectrometer. Briefly, corneal tissues from *C. albicans*-infected mice and negative controls (mock inoculated with sterile PBS) were collected for protein extraction followed by digestion with an enzyme to produce peptides. Afterwards, peptide mixture separation was performed with the UPLC system (analytical column: Acclaim™ Pepmap™ C18, 0.2 μm, 100 Å, 75 μm × 25 cm; trap column: Acclaim™ Pepmap™ C18, 3 μm, 75 μm × 2 cm; mobile phase: A: 0.1% formic acid in water; B: 0.1% formic acid in acetonitrile). Mass spectrometry was conducted under the following conditions: Tune: Spray voltage 2.1 kV, Capillary temperature: 320 °C; Full MS: Resolution 120,000@m/z 200, RF lens: 40%, AGC target: 4e5, Max IT: 50 ms, Scan range: m/z 350–1500; MS/MS: Intensity threshold: 1e4, Charge state: 2–7, Dynamic exclusion: 60 s, AGC target: 2e4, Max IT: 10 ms, Isolation window: 1 Da, Collision energy: 30% HCD, Scan range: m/z 200–1400.

Raw mass spectrometry data were analysed using Proteome Discoverer 2.5 (Thermo Fischer Scientific) and were subjected to protein identification against the reviewed UniProt *Mus musculus* (mouse) database (including 17,030 proteins). We defined a twofold increase or 0.5-fold decrease and p value < 0.05 as the threshold for different proteins. GO (Gene Ontology) enrichment analysis and KEGG pathway enrichment analysis for these dysregulated proteins were performed.

TLR4- and GSDMD-knockout mice

To generate TLR4- or GSDMD-knockout mice, this project used CRISPR/Cas9 technology to introduce mutations by nonhomologous recombination repair, causing a frameshift of the TLR4 (or GSDMD) gene. In brief, the procedure was as follows: Cas9 mRNA and gRNA were obtained by in vitro transcription, and F0 generation mice were microinjected into the fertilized eggs of C57BL/6 J mice. Confirmation by PCR product sequencing yielded F0 mice frameshifted for the target gene protein, and F0 strains were mated with C57BL/6 J mice for positive F1 mice. All experimental mice in this research were bred and maintained in a specific pathogen-free (SPF) house. Sequencing was used for genotyping TLR4- or GSDMD-knockout mice. The primers were as follows:mTLR4-Wild-type allele

Forward: 5'-AGCAAAGACAAGGGAGTAAGAA-3',
Reverse: 5'-GCCTGAAATACTGGCTAAAAG-3';
mTLR4-Mutant allele
Forward: 5'-GTCCCTGATGACATTCCTTCT-3',
Reverse: 5'-CTGTTTCTTGCCCATAGTTGA-3';
mGSDMD Forward: 5'-CGATGGAACGTAGTGCTG TG-3';
Reverse: 5'-TCCTTCCCAACCTGCTGTTG-3'.

Clinical scoring

Animals were scored for the severity of fungal keratitis (FK) with a dissecting microscope and a slit lamp. A grade of 0 to 4 was assigned to each mouse following the three criteria: area of opacity, density of opacity, and surface regularity [33]. Normal, unscratched mouse corneas were scored of 0 in each category, resulting in an overall score of 0. All three categories for each eye were scored daily, with a possible total score between 0 and 12. A total score of 5 or less was considered mild eye disease, a total score of 6 to 9 was categorized moderate eye disease, and a total score of more than 9 was considered severe eye disease.

Macrophage culture and treatment

RAW264.7 macrophages (#CTCC-001-0048, MeisenCTCC, Zhejiang, China) were cultured in DMEM (#C11995500BT, Gibco, USA) supplemented with 10% foetal bovine serum (#10,099,141, Gibco, USA) and 1% penicillin−streptomycin (#15,140,122, Gibco, USA) at 37 °C in 5% CO_2. When the cells reached 60–80% confluence, they were treated with 1×10^6 CFU/mL *C. albicans* suspension or 100 ng/ml mouse recombinant S100A8/A9 protein (#RPK504Mu01, CloudClone, Wuhan, China) for 24 h. After harvesting, the cells were lysed in RIPA buffer (#R0010, Solarbio, China) for total protein extraction and were lysed in TRIzol reagent (Invitrogen, USA) for RNA extraction.

Quantitative real-time PCR (RT−qPCR)

Total RNA from mouse corneas was extracted by TRIzol reagent (Invitrogen, USA) and quantified by Thermo Nanodrop 2000 spectrophotometry. One microgram of RNA was used to produce a cDNA template for PCR using a reverse transcription kit (#1,708,891, Bio-Rad, USA). cDNA was amplified via iTaq Universal SYBR® Green Supermix (#1,725,121, Bio-Rad, USA) on a quantitative real-time PCR instrument (Light Cycler 480II, Roche, Switzerland). The mRNA levels of specific genes were normalized against the reference gene GAPDH using the comparative Ct method ($2^{-\Delta\Delta Ct}$). The primers sequence used in this study are shown in Supplementary Table 1 (see Supplementary file 1).

Western blotting

Total proteins extracted from mouse corneas or RAW264.7 macrophages were measured by the BCA protein assay kit (#23,227, Thermo Scientific, USA). Extracted proteins were then separated on 4–20% Mini-PROTEAN Precast Gels (#456-1094, Bio-Rad, USA) and transferred onto polyvinylidene difluoride (PVDF) membranes (0.2 μm pore size; #ISEQ00010, Millipore, USA) or nitrocellulose membranes (0.45 μm pore size; Merck, USA). The membranes were blocked with NcmBlot Blocking Buffer (NCM Biotech) for 10 min at room temperature and then incubated with primary antibodies at 4 °C overnight. Primary antibodies targeting S100A8 (1:250; #MAB3059, R&D systems), S100A9 (1:500; #ab242945, Abcam), TLR4 (1:500; #ab13556, Abcam), NLRP3 (1:500; #ab263899, Abcam), cleaved CASP1 (1:250; #89,332, Cell Signaling Technology), ASC (1:250; #sc-514414, Santa Cruz Biotechnology), GSDMDC1 (1:250; #sc-393581, Santa Cruz Biotechnology), and β-actin (1:1000; #AC026, ABclonal) were used in this study. Subsequently, the membranes were incubated with HRP-conjugated secondary antibodies (1:1000) at room temperature for 1 h and detected with enhanced chemiluminescence (ECL) reagent (#32,106, Thermo Scientific, USA). To perform densitometry analysis, digital images of the positive bands were analysed using the image analysis software ImageJ 1.48.

Immunohistochemical/immunofluorescence staining

For immunohistochemical staining, mouse corneal sections or RAW264.7-cell climbing slices were deparaffinized in xylene and then dehydrated in gradient ethanol. Sections were filled with EDTA buffer in the microwave oven to repair antigen. To block nonspecific binding, 3% bovine serum albumin (BSA) was added to cover the tissue for 30 min. The samples were then incubated with primary antibodies (diluted with BSA appropriately) overnight at 4 °C, followed by incubation with secondary antibodies at room temperature for 50 min in the dark. Nuclei were labelled with 4,6-diamido-2-phenylindole dihydrochloride (DAPI). Spontaneous fluorescence quenching reagent was added and incubated for 5 min. At last, the photographs were taken with a Nikon imaging system (Nikon DS-U3, Nikon, Japan). The primary antibodies were as follows: anti-S100A8 + S100A9 (1:100; #ab288715, Abcam), anti-S100A8/A9 complex (1;100; #ab22506, Abcam), anti-CD68 (1:100; #ab283654, Abcam), anti-F4/80 (1:100; #ab90247, Abcam), anti-NLRP3 (1:100; #GB11300, Wuhan Servicebio Technology Co., Ltd.), and anti-GSDMDC1 (1:100, #sc-393581; Santa Cruz Biotechnology).

Treatment regimen

After intraperitoneal injection system anaesthesia, mice were subconjunctivally injected with 10 μL of mS100A8 siRNA (50 nM, Ribobio, #siBDMV002), 10 μL of mNLRP3 siRNA (50 nM, Ribobio, #siBDMV002), 10 μL of mouse recombinant S100A8/A9 protein (1000 ng/mL, CloudClone, #RPK504Mu01), 10 μL of paquinimod (2 μg/μL, MCE, #ABR25757), or 10 μL of azeliragon (2 μg/μL, MCE, #HY50682) twice at 24 h and 6 h before *C. albicans* infection. Additionally, 2 μL of siRNA (mS100A8 siRNA or mNLRP3 siRNA), mouse recombinant S100A8/A9 protein, paquinimod, or azeliragon was topically administered to the mouse eyes in the treated group four times per day.

Statistics

GraphPad Prism 6.0 software program (GraphPad Software, Inc. United States) was used for statistical analysis. All experiments were conducted at least three times independently. The data are presented as the mean ± standard error of the mean (SEM) and were analysed by Student's t test or one-way ANOVA post Dunnett's post hoc test.

A p value < 0.05 was considered to indicate statistical significance.

Results

C. albicans infection induces aberrant expression of the alarmin S100A8/A9 in mouse corneas

To characterize the early immune responses during fungal keratitis (FK) in depth, we infected mouse corneas with *C. albicans* and performed quantitative proteomics analysis on corneas collected from infected and mock-infected mice at Day 1 postinfection (dpi). A total of 498 proteins were significantly upregulated (fold change > 2, p value < 0.05), and 860 proteins were downregulated (fold change < 0.5, p value < 0.05) in *C. albicans*-infected mouse corneas compared with mock-infected corneas (Fig. 1A). GO analysis of upregulated proteins demonstrated an enrichment in several biological processes associated with *C. albicans* keratitis, such as the innate immune response, inflammatory response, and programmed cell death (Fig. 1B). Given

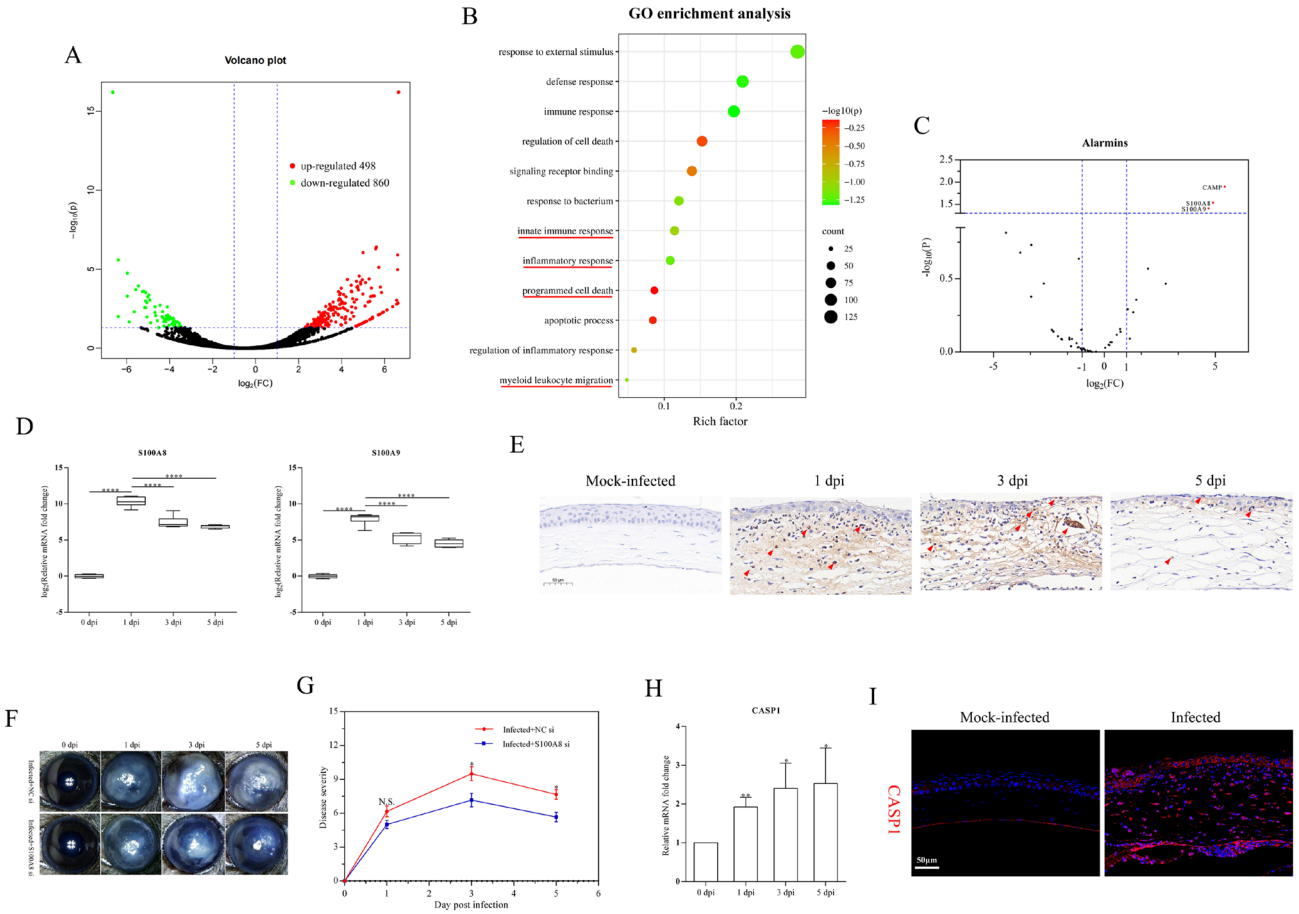

Fig. 1 Alarmin S100A8/A9 is significantly induced at the early stage of *C. albicans* keratitis. **A** Volcano plots showing differentially expressed proteins in mouse corneas infected with *C. albicans* at 1 dpi. Expression of 498 proteins was significantly upregulated, and the expression of 860 proteins was downregulated in the infected group compared with the mock infected. Fold change > 2 or < 0.5, p value < 0.05 was statistically significant. **B** Go analysis of the upregulated proteins in mouse corneas infected with *C. albicans* compared with mock (fold change > 2, p value < 0.05). **C** Scatter plot showing that S100A8 and S100A9 were the most significantly induced proteins among the all known alarmins at 1 dpi (fold change > 2, p value < 0.05). **D** Correlation between disease progression and S100A8/A9 mRNA expression in *C. albicans*-infected mice. One-way ANOVA post hoc Dunnett's test, $n = 6$, data are presented as the mean ± SEM, $^{****}p < 0.0001$. **E** Immunohistochemical analysis of the location and expression of S100A8/A9 in the cornea tissue of mock-infected and infected mice at 1, 3, 5 dpi. S100A8/A9 complex was increased significantly both in the stroma and epithelium of the corneas exposed to C. albicans. The red arrows indicate the S100A8/A9^{+} signals. Scale bars, 50 μm. **F** and **G** Representative images and quantitative analysis of cornea defects of infected mice treated with negative control siRNA (NC si) or S100A8 siRNA (S100A8 si). Student's t test, $n = 6$, data are presented as the mean ± SEM, $^{*}p < 0.05$, N.S. means no significant difference. (H) RT−qPCR analysis for the mRNA expression of CASP1 at 0, 1, 3, 5 dpi. Student's t test, $n = 3$, data are presented as the mean ± SEM, $^{*}p < 0.05$, $^{**}p < 0.01$. (I) Representative images of fluorescent staining targeting CASP1 in corneas of mock-infected and infected mice at 1 dpi. Scale bars, 50 μm

that alarmins are pivotal participants in the innate immunity of the host against microbial invasion, we subsequently focused on all known alarmins and noticed that two calcium-binding proteins termed S100A8 and S100A9 were markedly upregulated (fold change 29.8 and 25.9, respectively, p value < 0.05) at 1 dpi (Fig. 1C). The protein abundance obtained using label-free protein quantification methods was further validated by Western blotting, revealing that S100A8 and S100A9 protein expression increased with time in mouse corneas after *C. albicans* infection, reached a maximum at 1 dpi, and began to decrease thereafter (Figs. S1A and S1B, see Supplementary file). Afterwards, RT−qPCR analysis indicated that the mRNA expression levels of S100A8 and S100A9 were closely associated with the progression of *C. albicans* keratitis (Fig. 1D), wherein S100A8 and S100A9 may provide an early alarm signal for the disease. Since extracellular S100A8 and S100A9 function in the form of heterodimer proteins, immunohistochemistry staining was performed to detect the S100A8/A9 complex in mouse corneas. The results revealed that elevated S100A8/A9 complex signals were observed both in the stroma and epithelium of the corneas exposed to *C. albicans* but not in the mock-infected group (Fig. 1E). To probe the precise function of S100A8/A9 in *C. albicans* keratitis, we knocked down S100A8/A9 in infected corneas by subconjunctival injection of S100A8 small interfering RNA (S100A8-siRNA) (Fig. S3A, see Supplementary file). Decreased expression of S100A8/A9 not only reduced the density of corneal opacity but also attenuated the opacity area in the infected corneas, especially in the middle phase (3 and 5 dpi) (Fig. 1F and G), implying that S100A8/A9 serves as a critical factor contributing to the pathogenesis of *C. albicans* keratitis. In addition to S100A8 and S100A9, CASP1 was also screened by proteomics analysis and validated at the mRNA and protein levels in the FK model (Fig. 1H and I). CASP1 is an indicator of NLRP3 inflammasome activation, suggesting the involvement of S100A8/A9 in *C. albicans* keratitis by inducing NLRP3 inflammasome production. However, this hypothesis requires further experimental confirmation.

C. albicans keratitis is characterized by S100A8/A9 driving NLRP3 inflammasome activation

Elevated levels of NLRP3, ASC, and cleaved CASP1 protein were observed in corneas following *C. albicans* infection in our previous study [27], implying the contribution of the NLRP3 inflammasome signalling pathway to the pathogenesis of FK. The S100A8/A9 blocker paquinimod, which inhibits the interaction of extracellular S100A8/A9 with its receptors (TLR4 and RAGE) on the cell surface, was used to explore the role of S100A8/A9 in mouse corneal NLRP3 inflammasome activation against *C. albicans* infection. The results verified that the corneas treated with the S100A8/A9 blocker exhibited a reduced severity level compared to vehicle-treated corneas, evidenced by a significant decrease in clinical scoring (Fig. 2A and B). Notably, the S100A8/A9 inhibitor significantly suppressed the mRNA increase in NLRP3 and CASP1 but not ASC (Fig. 2C), indicating that S100A8/A9 might provide a prime signal for NLRP3 inflammasome activation in FK. Western blotting showed dramatically decreased expression of NLRP3, ASC, and cleaved CASP1 protein in the infected corneas following S100A8/A9 inhibition (Fig. 2D and E). Immunofluorescence and immunohistochemistry staining data revealed that diminished NLRP3 was accompanied by decreased macrophages ($CD68^+$) in infected mouse corneas when S100A8/A9 was inhibited (Fig. 2F and G), which further demonstrated S100A8/A9 functions via NLRP3 inflammasome activation in *C. albicans* keratitis. These findings link S100A8/A9 to its downstream NLRP3 inflammasome signal; however, the specific functional component between S100A8/A9 and NLRP3 inflammasome activation remains unclear.

TLR4 is required for S100A8/A9-induced NLRP3 inflammasome activation in *C. albicans* keratitis

Among the PRRs identified on the cell surface, TLR4 and RAGE are two major PRRs that are believed to be responsible for S100A8/A9 recognition [34]. GO enrichment for different proteins also showed that S100A8 was closely related to TLR4 binding in *C. albicans* keratitis (Fig. S4, see Supplementary file). We found that the expression of TLR4 mRNA was significantly upregulated in mouse corneas as early as 1 dpi, although the change in RAGE expression was not statistically significant (Fig. 3A). Further immunofluorescent staining targeting TLR4 revealed that the TLR4 protein was mainly located in the corneal stroma and epithelium after fungal infection (Fig. 3B), indicating that TLR4 is activated during *C. albicans* keratitis. Therefore, we explored the role of TLR4 in the S100A8/A9-NLRP3 pathway in *C. albicans* keratitis using TLR4-knockout mice. The results showed that ablating TLR4 significantly alleviated disease severity (Fig. 3C and D) and simultaneously suppressed the expression of NLRP3 and CASP1 at both the protein and mRNA levels (Fig. 3E–G) in *C. albicans*-infected mouse corneas. Our results also proven that NLRP3 protein expression was significantly decreased in the corneal epithelium and stroma of TLR4-deficient mice, evidenced by the immunofluorescent staining (Fig. 3H). In addition, it is known that S100A8/A9 is also implicated in the RAGE pathway; nevertheless, whether RAGE is engaged in NLRP3 inflammasome activation in *C. albicans* keratitis is not well understood. To figure. this out, we treated mice infected with *C. albicans* with the RAGE signalling inhibitor azeliragon. The data showed that inhibiting RAGE pathway did not markedly prevent the production of NLRP3, ASC, or cleaved

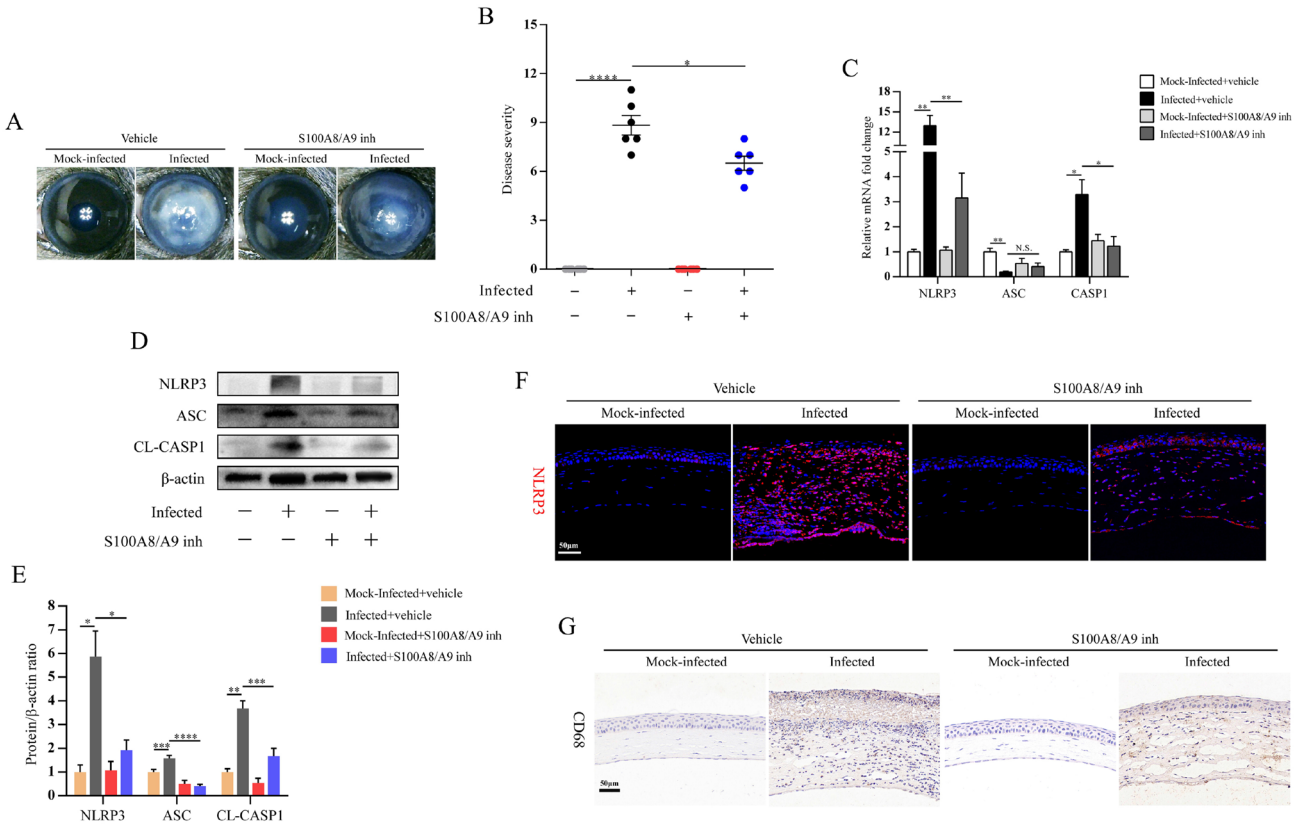

Fig. 2 Inhibiting S100A8/A9 attenuates *C. albicans* keratitis progression by preventing the activation of NLRP3 inflammasome. **A** and **B** Representative images and quantitative analysis of cornea defects of mock-infected and infected mice treated with vehicle or S100A8/A9 inhibitor (inh) at 2 dpi. $n=6$. **C** Inhibition of S100A8/A9 significantly decreased mRNA expression of NLRP3 and CSAP1 in vivo at 2 dpi. $n=3$. **D** and **E** S100A8/A9 regulated the protein expression of NLRP3, ASC and cleaved CASP1 (CL-CASP1) in vivo at 2 dpi. $n=3$. The protein bands were normalized to β-actin and the mock-infected group was taken as the calibrator. **F** and **G** Fluorescent or immunohistochemical analysis of the location and expression of NLRP3 or CD68 in the cornea tissue of mock-infected and infected mice treated with vehicle or S100A8/A9 inhibitor at 2 dpi. Scale bars, 50 μm. Student's *t* test, data are presented as the mean ± SEM, $*p<0.05$, $**p<0.01$, $***p<0.001$, $****p<0.0001$, N.S. means no significant difference

CASP1 protein (Fig. 3K and L), while the corneal opacity deficit was not significantly attenuated, as evidenced by clinical scoring (Fig. 3I and J). These loss-of-function studies reflected that TLR4, not RAGE, was needed for S100A8/A9-mediated NLRP3 inflammasome activation in FK.

Macrophage pyroptosis facilitates S100A8/A9 release in an NLRP3-dependent manner

Cell rupture causes the release of the cytokines IL-1β and IL-18 and alarmins, signifying the inflammatory potential of pyroptosis [35, 36]. Our previous studies have proven that the maturation of the pyroptosis effector molecule GSDMD is dependent on NLRP3 inflammasome activation in *C. albicans* keratitis. In the present study, F4/80-positive macrophages costained with GSDMD were detected in FK mouse corneas, as evidenced by the immunofluorescent staining data (Fig. 4A), implying that mature macrophage pyroptosis is involved in *C. albicans* keratitis. To further probe the molecular nature of S100A8/A9 production in mouse corneas against *C. albicans* invasion, we next built a FK model using GSDMD-knockout mice, followed by monitoring the expression levels of S100A8/A9 by Western blotting and RT−qPCR. The experimental results indicated that genetic deletion of GSDMD led to diminished S100A8/A9 protein and mRNA levels (Fig. 4B–D), accompanied by the attenuation of inflammation in mouse corneal tissues (Fig. 4E and F). Further immunofluorescent staining results showed that GSDMD deficiency caused a reduction in S100A8/A9-positive macrophages in FK mouse corneas (Fig. 4G), which together suggests that macrophage pyroptosis is a key determinant in S100A8/A9 processing. We next investigated the role of NLRP3 in S100A8/A9 production by inhibiting NLRP3 expression via small interfering RNA (NLRP3-siRNA). The results demonstrated that the knockdown of NLRP3 resulted in an apparent decrease in the levels of S100A8/A9 both at the mRNA and protein levels (Fig. 4H–J). Mice with NLRP3 deficiency had attenuated

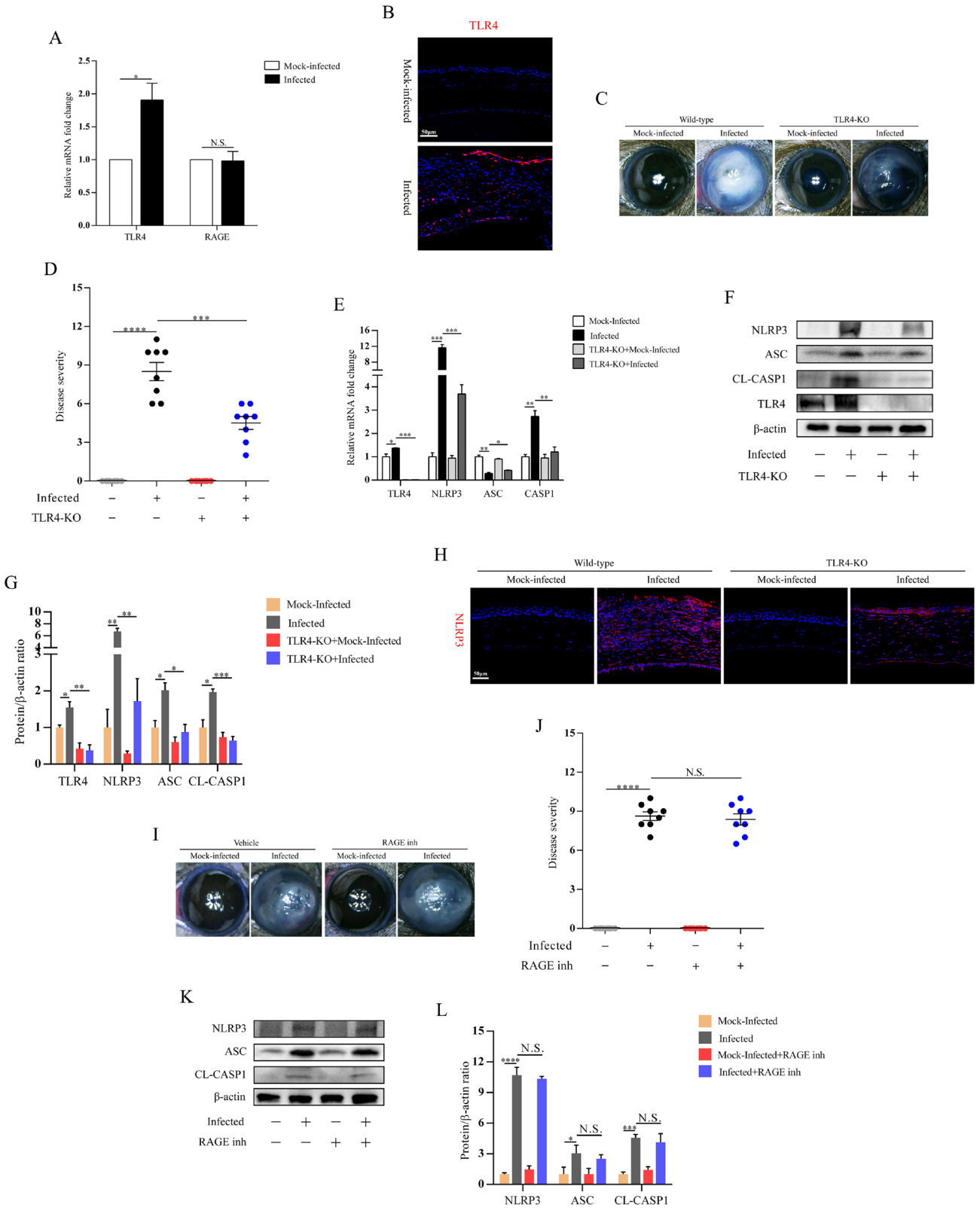

corneal disease severity compared to wild-type mice (Fig. 4K and L). Immunofluorescence staining revealed that silencing NLRP3 not only inhibited S100A8/A9 expression but also decreased the accumulation of GSDMD-positive mature macrophages in FK (Fig. 4M). All these results demonstrated that macrophage pyroptosis promoted S100A8/

◂**Fig. 3** S100A8/A9-induced NLRP3 inflammasome activation is dependent on TLR4 in *C. albicans* keratitis. **A** RT−qPCR analysis for the mRNA expression of TLR4 and RAGE in mock-infected and infected mouse corneas at 1 dpi ($n=3$). **B** Fluorescent staining analysis showing TLR4 was increased in mouse corneas after *C. albicans* infection at 1 dpi. Scale bars, 50 μm. **C** and **D** Representative images and quantitative analysis of cornea defects of wild-type and TLR4-KO mice infected with *C. albicans* at 2 dpi. $n=8$. **E–G** Western blotting and RT−qPCR analysis detecting mRNA and protein levels of NLRP3 inflammasome in wild-type and TLR4-KO mice treated with *C. albicans* at 2 dpi. $n=3$. The protein bands were normalized to β-actin and the mock-infected group was taken as the calibrator. **H** Fluorescent staining analysis of the location and expression of NLRP3 in the cornea tissue of wild-type and TLR4-KO mice treated with *C. albicans* at 2 dpi. Scale bars, 50 μm. **I** and **J** Representative images and quantitative analysis of cornea defects of mock-infected and infected mice treated with vehicle or RAGE inhibitor (inh) at 2 dpi. $n=8$. **K** and **L** Western blotting analysis detecting protein levels of NLRP3 inflammasome in mock-infected and infected mice treated with vehicle or RAGE inhibitor at 2 dpi. $n=3$. The protein bands were normalized to β-actin and the mock-infected group was taken as the calibrator. Student's t test, data are presented as the mean ± SEM, $^{*}p<0.05$, $^{**}p<0.01$, $^{***}p<0.001$, $^{****}p<0.0001$, N.S. means no significant difference

A9 release during FK, and this process was dependent on NLRP3 inflammasome activation.

S100A8/A9 amplifies inflammatory responses by forming a positive feedback loop with the NLRP3 inflammasome

As described above, macrophage pyroptosis facilitates the production of the alarmin S100A8/A9 in *C. albicans*-infected corneas. Then, what is the effect of S100A8/A9 on macrophages themselves? To address this issue, we first overexpressed S100A8/A9 in both mock-infected and *C. albicans*-infected mouse corneas by subconjunctival injection of mouse recombinant S100A8/A9 (r-S100A8/A9). As shown in Fig. 5A and B, after *C. albicans* infection, the mean score of disease severity in the group with r-S100A8/A9 was markedly higher than that in the group with PBS, whereas no significant defects were detected in the mock-infected group with r-S100A8/A9, indicating that r-S100A8/A9 administration could worsen corneal defects under *C. albicans* infection. Next, we examined the levels of NLRP3, ASC, and cleaved CASP1 in corneas with or without re-S100A8/A9 at 2 dpi by Western blotting and found that the overexpression of S100A8/A9 could promote NLRP3, ASC, and cleaved CASP1 expression in *C. albicans*-infected corneas rather than mock-infected corneas (Fig. 5C and D). Further immunofluorescent staining also verified that NLRP3 expression was markedly increased in corneas when mice were subconjunctivally injected with r-S100A8/A9 one day before fungal infection (Fig. 5E). We next investigated the effects of S100A8/A9 on macrophage NLRP3 inflammasome activation in vitro using the mouse macrophage cell line RAW264.7. After 24 h of coculture with *C. albicans*, the protein expression levels of NLRP3, ASC, and cleaved CASP1 increased in RAW264.7 cells (Fig. 5F and G). Further study showed that exogenous administration of r-S100A8/A9 led to elevated NLRP3, ASC, and cleaved CASP1 protein in both *C. albicans*-infected and uninfected macrophages (Fig. 5F and G). Immunofluorescence staining data provided evidence that more NLRP3-positive macrophages were seen in the r-S100A8/A9-treated cells than in the control cells (Fig. 5H). These results, together with the previous results, reflected that S100A8/A9 had the ability to induce its own production by promoting NLRP3/GSDMD-mediated macrophage pyroptosis, thereby forming a positive loop and amplifying the aberrant immunity responses in *C. albicans* keratitis (Fig. 6).

Discussion

As one of the leading causes of corneal blindness worldwide, fungal keratitis has become an increasingly serious threat to public ocular health without the availability of effective treatment strategies [37]. Among the pathogenic fungi involved in keratitis, *C. albicans* has been identified as one of the dominant pathogens, especially in Europe and America [38]. *C. albicans* specifically penetrates the corneal stroma after a transition from yeasts into filamentary forms, which disrupts the ocular surface defence and leads to corneal inflammation and ulceration [39]. Following fungal invasion, various alarmin molecules (also known as damage-associated molecular patterns, DAMPs) released from stressed or damaged cells relay intracellular defence signals by interacting with pattern recognition receptors (PRRs) to activate innate immune responses [40]. The fine tuning of alarmin expression is essential for maintaining immune homeostasis; however, its aberrant expression can be deleterious to corneas, triggering a cytokine storm or excessive inflammatory responses. Therefore, finding a balance between eliminating pathogenic fungi and reducing inflammatory damage in corneas is a subject worthy of intensive investigation.

To elucidate the molecular mechanism underlying *C. albicans* keratitis, a diverse spectrum of alarmin molecules was investigated by quantitative proteomics based on LC−MS/MS. Herein, our research found that S100A8 and S100A9 were two major upregulated alarmins at the early stage (1 dpi) of *C. albicans* keratitis, and the changes in their expression tightly correlated with the disease process, qualifying the protein as a reliable biomarker for corneal inflammation. Notably, the S100A8/A9 complex was detectable either within or outside the cells after *C. albicans* corneal infection, which further validates that extracellular S100A8/A9 serves as a warning signal for the host in the

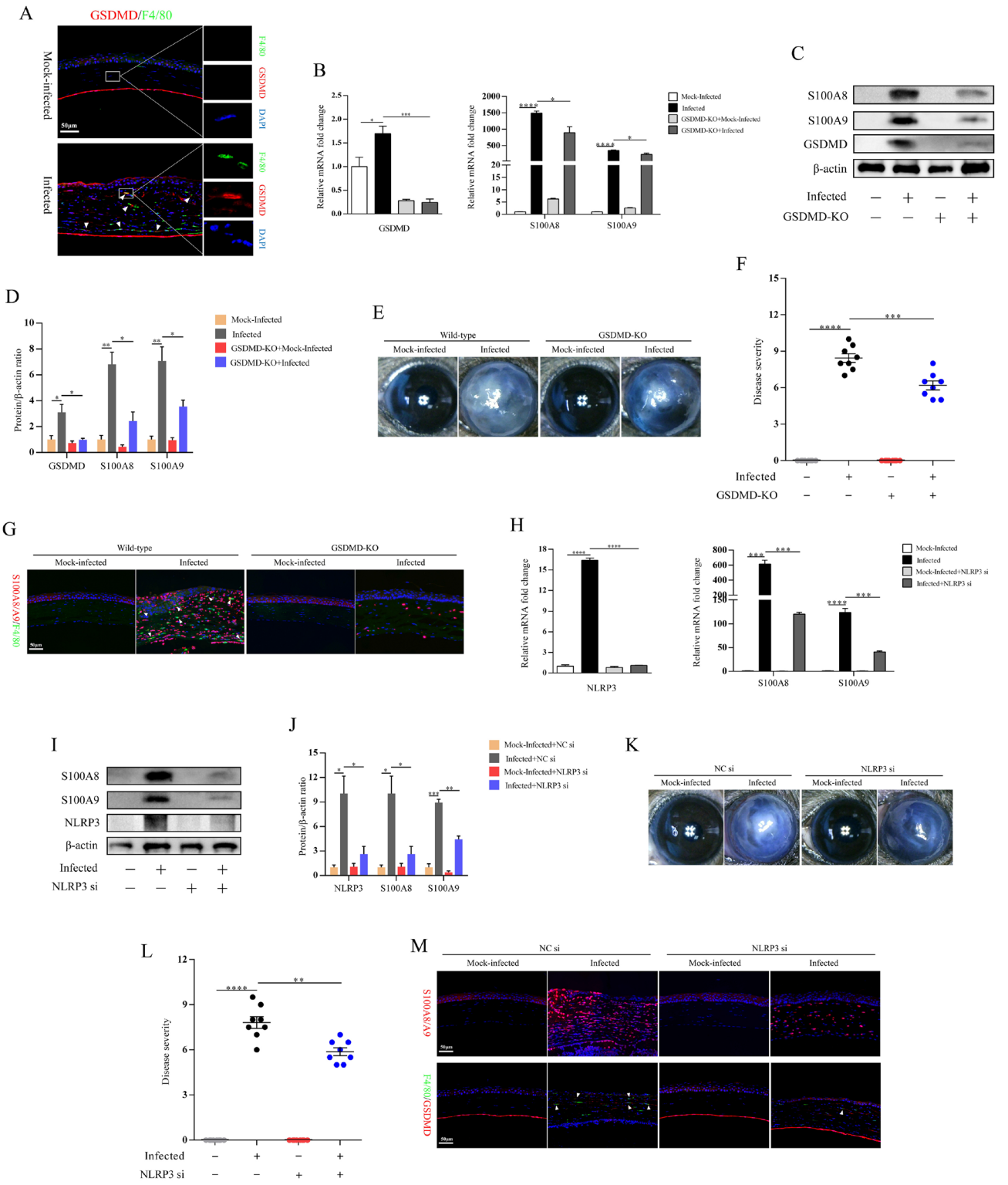

form of heterodimers. In addition to its expression in myeloid cells, S100A8/A9 is reported to be found in keratinocytes and epithelial cells under inflammatory conditions [41, 42]. Currently, most of the positive staining for S100A8/A9 was located in the corneal stroma, but they were also observed in the epithelium after *C. albicans* infection. This finding indicates that corneal epithelial cells contribute to the source of S100A8/A9 against fungal stimulation. Unfortunately, to date, the specific cell source of S100A8/A9 has not been completely defined in *C. albicans* keratitis, and we

◂**Fig. 4** Macrophage pyroptosis promotes S100A8/A9 release in a NLRP3-dependent manner during *C. albicans* keratitis. **A** Representative images of fluorescent staining targeting F4/80 (mature macrophage maker) and GSDMD in mock-infected and infected mouse corneas. The white arrows indicate the $GSDMD^+$ macrophages. Scale bars, 50 μm. **B–D** Knockout of GSDMD markedly decreased the mRNA and protein levels of S100A8/A9 in mouse corneas infected with *C. albicans* at 2 dpi. $n=3$. The protein bands were normalized to β-actin and the mock-infected group was taken as the calibrator. **E** and **F** Representative images and quantitative analysis of cornea defects of wild-type and GSDMD-KO mice infected with *C. albicans*. $n=8$. **G** Fluorescent staining showing ablating GSDMD led to decrease of $S100A8/A9^+$ macrophages (white arrows) in the infected mouse corneas at 2 dpi. Scale bars, 50 μm. **H–J** Western blotting and RT−qPCR analysis showing that knockdown of NLRP3 prevented the production of S100A8/A9 in mouse corneas infected with *C. albicans* at 2 dpi. $n=3$. The protein bands were normalized to β-actin and the mock-infected group was taken as the calibrator. **K** and **L** Representative images and quantitative analysis of cornea defects of mock-infected and infected mice treated with NC or NLRP3 siRNA. $n=8$. **M** Fluorescent staining analysis showing that silencing NLRP3 decreased both S100A8/A9 and $GSDMD^+$ macrophages (white arrows) in the infected mouse corneas. Scale bars, 50 μm. Student's *t* test, data are presented as the mean ± SEM, $^*p<0.05$, $^{**}p<0.01$, $^{***}p<0.001$, $^{****}p<0.0001$

believe that single-cell sequencing will serve to resolve the contribution of individual cells to S100A8/A9. In addition to S100A8 and S100A9, CAMP (cathelicidin antimicrobial peptide) was another alarmin molecule which markedly increased in infected corneas by LC−MS/MS analysis (Fig. 1C). Our previous study has demonstrated that CAMP might possess antimicrobial activity in *C. albicans* keratitis [43]. It is reported S100A8/A9 exhibits broad-spectrum antimicrobial activity by its ability to chelate Zn^+ and Mn^+ [44, 45]. A study by Clark HL et al. revealed that neutrophils from S100A9 deficiency mice have an impaired ability to inhibit hyphal growth in vitro, and in infected corneas from *Aspergillus fumigatus* (*A. fumigatus*) keratitis mouse models [46]. Whether S100A8/A9 performs a similar function in *C. albicans* keratitis is unknown until now. This question warrants continuing investigations in the future.

The NLRP3 inflammasome is critical for host defences against bacterial, fungal, and viral infections [47]. Two signals have been proposed for NLRP3 inflammasome activation. The priming signal is provided by microbial components or endogenous danger molecules, leading to the activation of the transcription factor NF-κB and subsequent upregulation of NLRP3 [48, 49]. Our previous work demonstrated that NLRP3 inflammasome activation was engaged in the pathogenesis of *C. albicans* keratitis [27]. In the present research, we found that inhibiting S100A8/A9 significantly downregulated NLRP3 and CASP1 expression at both the mRNA and protein levels, accompanied by improvement in fungal keratitis, indicating that alarmins S100A8/A9 are potent activators of the NLRP3 inflammasome during *C. albicans* keratitis. In addition, reduced corneal infiltration by $CD68^+$ macrophages was detected following S100A8/A9 blockade, which suggests that S100A8/A9 is engaged in macrophage activation. Curiously, the change of ASC at mRNA and protein levels are not consistent after *C. albicans* infection. Similar findings were also observed in our previous study, which discovered that ASC and IL-18 increased at protein levels but reduced at mRNA after *C. albicans* corneal infection [27]. Several interpretations may explain this issue. First, there are many complicated and varied post-transcriptional mechanisms involved in turning mRNA into protein that are not yet sufficiently well defined to be able to compute protein concentrations from mRNA [50, 51]. Second, factors, such as mRNA degradation, protein degradation, and folding of the expression, may also result in inconsistent mRNA abundance and protein expression levels [52, 53].

Acting as a crucial pattern recognition receptor, TLR4 recognizes lipopolysaccharide (LPS) or endogenous signals, including HMGB1 and S100A8/A9, which induce the release of proinflammatory cytokines that are necessary to activate potent immune responses [54, 55]. In addition, the activation of the NLRP3 inflammasome occurs through a prime signal provided by the activation of Toll-like receptors (TLRs), interleukin-1 (IL-1) receptors, or tumour necrosis factor receptors (TNFRs) [56, 57].

Our results showed that TLR4 expression significantly increased after *C. albicans* infection, and the protein levels of NLRP3, ASC, and cleaved CASP1 were diminished after TLR4 knockout in vivo, verifying that TLR4 activation is upstream of the NLRP3 inflammasome. Based on this, it is possible that S100A8/A9 contributes to the activation of TLR4 signalling, in turn providing danger signals to intracellular NLRP3. It is reported that HMGB1 Boxb exacerbates mice corneal inflammatory responses through the TLR4/MyD88-dependent signalling pathway in *A. fumigatus* keratitis [58]. Our previous genetic microarray analysis of *C. albicans* keratitis showed the mRNA of HMGB1 and HMGA2 significantly increased in the infected mouse corneas [59]. These results suggest us that TLR4 may have other ligands to delay intracellular signalling in addition to S100A8/A9 during *C. albicans* keratitis. Furthermore, RAGE is also believed to be a major receptor for S100A8/A9, and a recent study reported that S100A8/A9 promoted RAGE and carboxylated glycan-dependent activation of the MAPK and NF-κB signalling pathways in colon tumour cells [12, 60]. Therefore, we further explored the role of RAGE in *C. albicans* keratitis development using the inhibitor azeliragon. The results revealed that the inhibition of RAGE failed to prevent NLRP3 inflammasome formation and reduce the disease severity in the mouse models. Recently, glycosaminoglycans (GAGs) and EMMPRIN (CD147) were shown to be potential receptors for S100A8/A9 in melanoma cells [61, 62]. However, data

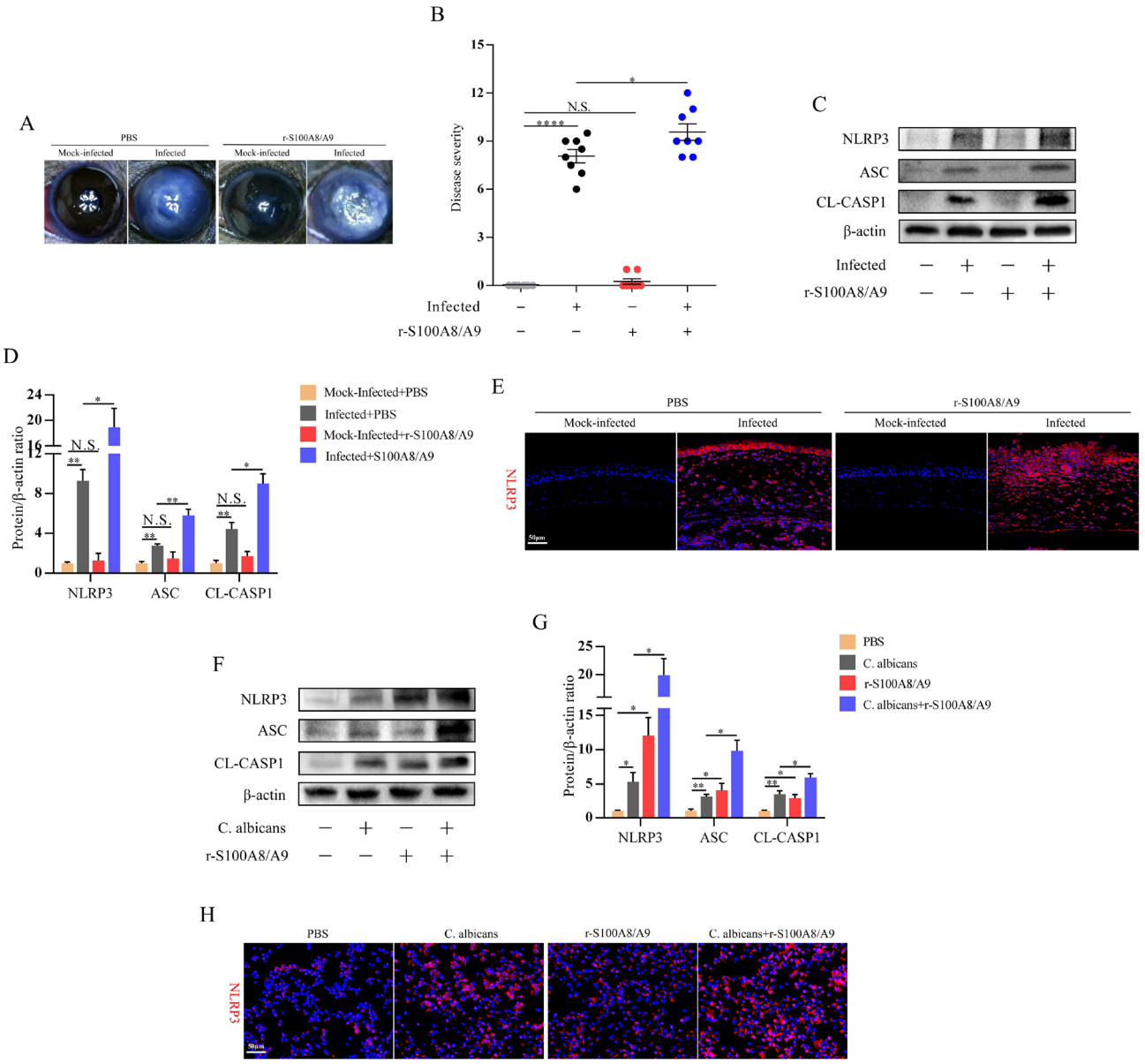

Fig. 5 S100A8/A9 worsens *C. albicans* keratitis by forming a positive feedback loop with NLRP3 inflammasome. **A** and **B** Representative images and quantitative analysis of mouse corneas treated with recombinant S100A8/A9 at 2 dpi ($n=8$). r-S100A8/A9: recombinant mouse S100A8/A9 protein. **C** and **D** Western blotting showing that the protein expression of NLRP3, ASC, and cleaved CASP1 significantly increased in the *C. albicans*-infected corneas at 2 dpi after r-S100A8/A9 treatment ($n=3$). The protein bands were normalized to β-actin and the mock-infected group was taken as the calibrator. **E** Representative images of fluorescent staining targeting NLRP3 in mock-infected and infected mouse corneas treated with r-S100A8/A9 at 2 dpi. Scale bars, 50 μm. **F** and **G** Western blotting showing that NLRP3, ASC, and cleaved CASP1 protein expression in RAW 264.7 cells after 24 h of *C. albicans* and r-S100A8/A9 administration ($n=3$). The protein bands were normalized to β-actin and the mock-infected group was taken as the calibrator. **H** Representative images of fluorescent staining targeting NLRP3 in RAW 264.7 cells after 24 h of *C. albicans* and r-S100A8/A9 administration. Scale bars, 50 μm. Student's *t* test, data are presented as the mean ± SEM, $*p<0.05$, $**p<0.01$, $****p<0.0001$, N.S. means no significant difference

confirming the functional relevance of this interaction in *C. albicans* keratitis are still lacking. In future studies, further investigation of the role of other pattern recognition receptors in addition to TLR4 and RAGE in corneal tissue is highly desirable.

Alarmins can be released by membrane rupture due to pyroptosis, apoptosis, and other types of cell death. Emerging studies have shown that *C. albicans*-induced macrophage pyroptosis is due to physical disruption caused by hyphae and is NLRP3 inflammasome dependent

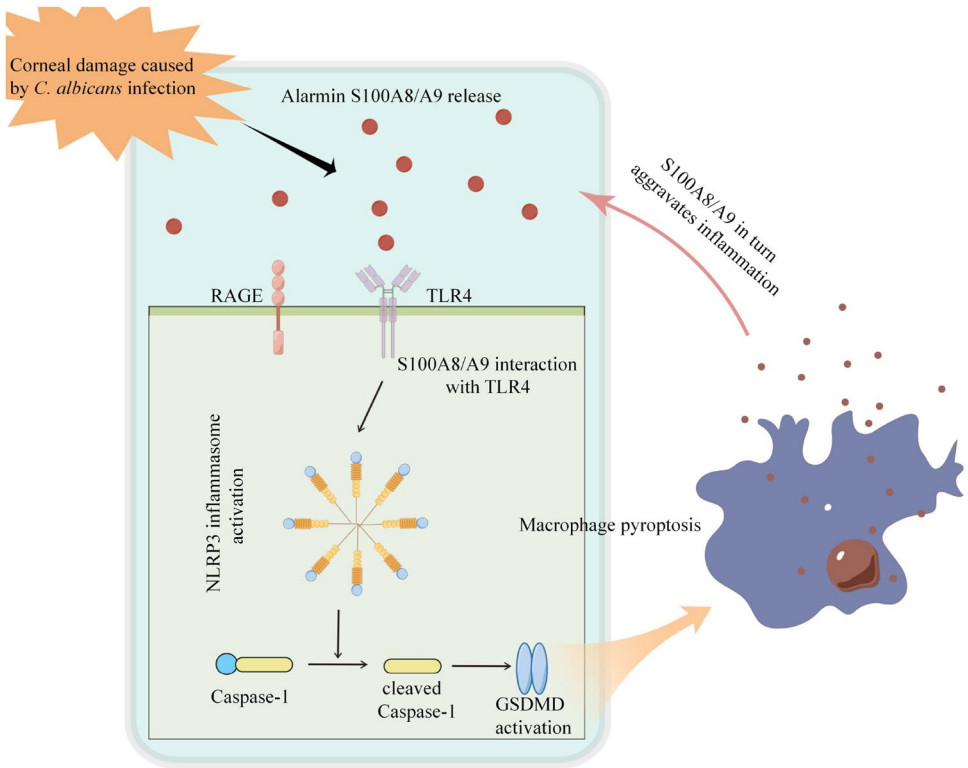

Fig. 6 Alarmin S100A8/A9 forms a positive feedback loop with NLRP3 inflammasome-GSDMD in the pathogenesis of *Candida albicans* keratitis

[63]. In the present study, we observed that upon knocking out GSDMD (a key effector of pyroptosis), the alarmin S100A8/A9 showed significant downregulation in *C. albicans* keratitis models. In addition, the colocalization of F4/80 and S100A8/A9 (or GSDMD) by immunofluorescence staining supports the idea that macrophage pyroptosis partially contributes to S100A8/A9 secretion. Further knockdown experiments in vivo showed that the release of the alarmin S100A8/A9 was dependent on NLRP3, which implies that macrophage NLRP3/GSDMD pathway activation is necessary for S100A8/A9 processing in *C. albicans* keratitis. Previous research revealed that monosodium urate crystals promoted macrophages that expressed S100A8/A9, and these S100A8/A9 further enhanced monosodium urate-induced NLRP3 inflammasome activation in macrophages, mediating the release of cytokine IL-1β in gout pain [64]. This result immediately suggested the involvement of S100A8/A9 in the positive feedback loop of the NLRP3-GSDMD axis in fungal keratitis. To verify this notion, we overexpressed S100A8/A9 in vivo and vitro and found that exogenous r-S100A8/A9 contributed to the exacerbation of fungal keratitis and the activation of the NLRP3 inflammasome. Curiously, in vivo NLRP3 inflammasome activation by exogenous S100A8/A9 has been hindered thus far in the absence of *C. albicans* infection. Therefore, we hypothesize that without a stimulus by fungal pathogen products (pathogen-associated molecular patterns, PAMPs), S100A8/A9 alone is unable to elicit the activation of the NLRP3 inflammasome in corneas, which is supported by a previous study that showed that under completely sterile conditions, DAMPs released following brain injury failed to induce inflammasome activation [65]. Additionally, we found that S100A8/A9 enhanced NLRP3, ASC, and cleaved CASP1 expression in RAW264.7 cells even without *C. albicans* stimulation in vitro. This result implied that after fungal pathogen invasion, extracellular S100A8/A9 signals to macrophages that have infiltrated the corneas to induce the NLRP3 inflammasome. In 2021, Ji QS et al. found human corneal epithelial cells-derived thymic stromal lymphopoietin (TSLP) could induce macrophages pyroptosis in *A. fumigatus* keratitis [66]. It gives us an indication that S100A8/A9 acts not only on macrophages itself but also upon corneal epithelial cells and other cells in cornea in response to *C. albicans* stimuli. That undoubtedly deserves further exploration in future studies.

In summary, our study validates the key roles of S100A8/A9 in *C. albicans* keratitis. Aberrant expression of S100A8/A9 magnifies the inflammatory response by promoting NLRP3 inflammasome activation, which induces a positive feedback loop and aggravates the keratitis. Macrophage pyroptosis facilitates the secretion of the alarmin S100A8/A9 in *C. albicans* keratitis, in which NLRP3-GSDMD pathway activation is a determinant. Moreover, we revealed that TLR4 but not RAGE relays the S100A8/A9 signal to intracellular NLRP3 in corneas against fungal challenge. These

results shed light on the characteristics of innate immunity in the pathogenesis of *C. albicans* infection and provide therapeutic targets for the treatment of fungal keratitis.

Supplementary Information The online version contains supplementary material available at https://doi.org/10.1007/s00011-023-01757-5.

Acknowledgements This study was funded by the National Natural Science Foundation of China (81970772 and 21906179), the National Key Research and Development Program of China (2020YFA0907500), the K.C. Wong Education Foundation of China (GJTD-2020-03), the Tianjin Natural Science Foundation (21JCZDJC01250), the Science and Technology Program of Baoding of Huifang Lian (No. 2141ZF086), and the Tianjin Key Medical Discipline (Specialty) Construction Project (TJYXZDXK-016A).

Author contributions XF was involved in investigation, methodology, writing—original draft, and writing—review and editing. HL, SL, JD, and WL contributed to investigation and methodology. XH performed writing—original draft, writing—review and editing, and supervision. CYL and XYY were involved in investigation, methodology, writing—original draft, writing—review and editing, and supervision. All the authors contributed to the revision of the final manuscript.

Availability of data and materials The datasets used and/or analysed during the current study are available from the corresponding author on reasonable request.

Declarations

Conflict of interest The authors have declared that no conflict of interest exists.

Ethics approval and consent to participate All animal experiments were in accordance with the ARVO Statement for the Use of Animals in Ophthalmic and Vision Research, and this study was formally reviewed and approved by the Research Centre for Eco-Environmental Sciences, Chinese Academy of Sciences Animal Care and Ethics Committee (Approval No. AEWC-RCEES-2022042).

References

1. Sharma N, Bagga B, Singhal D, Nagpal R, Kate A, Saluja G, et al. Fungal keratitis: a review of clinical presentations, treatment strategies and outcomes. Ocul Surf. 2021;24:22–30.
2. Prajna NV, Krishnan T, Mascarenhas J, Srinivasan M, Oldenburg CE, ToutainKidd CM, et al. Predictors of outcome in fungal keratitis. Eye (Lond). 2012;26:1226–31.
3. Mills B, Radhakrishnan N, Karthikeyan Rajapandian SG, Rameshkumar G, Lalitha P, Prajna NV. The role of fungi in fungal keratitis. Exp Eye Res. 2021;202: 108372.
4. Patin EC, Thompson A, Orr SJ. Pattern recognition receptors in fungal immunity. Semin Cell Dev Biol. 2019;89:24–33.
5. Santoni G, Cardinali C, Morelli MB, Santoni M, Nabissi M, Amantini C, et al. Danger- and pathogen-associated molecular patterns recognition by pattern-recognition receptors and ion channels of the transient receptor potential family triggers the inflammasome activation in immune cells and sensory neurons. J Neuroinflammation. 2015;12:21.
6. Zindel J, Kubes P. DAMPs, PAMPs, and LAMPs in immunity and sterile inflammation. Annu Rev Pathol. 2020;15:493–518.
7. Zhang X, Mosser DM. Macrophage activation by endogenous danger signals. J Pathol. 2008;214(2):161–78.
8. Shen H, Xu B, Yang C, Xue W, You Z, Wu X, et al. A DAMP-scavenging, IL-10-releasing hydrogel promotes neural regeneration and motor function recovery after spinal cord injury. Biomaterials. 2022;280: 121279.
9. Cunha C, Carvalho A, Esposito A, Bistoni F, Romani L. DAMP signaling in fungal infections and diseases. Front Immunol. 2012;3:286.
10. Wang S, Song R, Wang Z, Jing Z, Wang S, Ma J. S100A8/A9 in inflammation. Front Immunol. 2018;9:1298.
11. Pruenster M, Vogl T, Roth J, Sperandio M. S100A8/A9: From basic science to clinical application. Pharmacol Ther. 2016;167:120–31.
12. Volz HC, Laohachewin D, Seidel C, Lasitschka F, Keilbach K, Wienbrandt AR. S100A8/A9 aggravates post-ischemic heart failure through activation of RAGE-dependent NF-κB signaling. Basic Res Cardiol. 2012;107(2):250.
13. Gong T, Liu L, Jiang W, Zhou R. DAMP-sensing receptors in sterile inflammation and inflammatory diseases. Nat Rev Immunol. 2020;20(2):95–112.
14. Rigiracciolo DC, Nohata N, Lappano R, Cirillo F, Talia M, Adame-Garcia SR. Focal adhesion kinase (FAK)-Hippo/YAP transduction signaling mediates the stimulatory effects exerted by S100A8/A9-RAGE system in triple-negative breast cancer (TNBC). J Exp Clin Cancer Res. 2022;41(1):193.
15. Pirr S, Dauter L, Vogl T, Ulas T, Bohnhorst B, Roth J, Viemann D. S100A8/A9 is the first predictive marker for neonatal sepsis. Clin Trans Med. 2021;11(4): e338.
16. Joshi A, Schmidt LE, Burnap SA, Lu R, Chan MV, Armstrong PC. Neutrophil-derived protein S100A8/A9 alters the platelet proteome in acute myocardial infarction and is associated with changes in platelet reactivity. Arterioscler Thromb Vasc Biol. 2022;42(1):49–62.
17. van Bon L, Cossu M, Loof A, Gohar F, Wittkowski H, Vonk M. Proteomic analysis of plasma identifies the Toll-like receptor agonists S100A8/A9 as a novel possible marker for systemic sclerosis phenotype. Ann Rheum Dis. 2014;73(8):1585–9.
18. Guo Q, Zhao Y, Li J, Liu J, Yang X, Guo X, et al. Induction of alarmin S100A8/A9 mediates activation of aberrant neutrophils in the pathogenesis of COVID-19. Cell Host Microbe. 2021;29(2):222-235.e4.
19. Deng Q, Sun M, Yang K, Zhu M, Chen K, Yuan J, et al. MRP8/14 enhances corneal susceptibility to Pseudomonas aeruginosa Infection by amplifying inflammatory responses. Invest Ophthalmol Vis Sci. 2013;54(2):1227–34.
20. Skronska-Wasek W, Durlanik S, Le HQ, Schroeder V, Kitt K, Garnett JP, et al. The antimicrobial peptide S100A8/A9 produced by airway epithelium functions as a potent and direct regulator of macrophage phenotype and function. Eur Respir J. 2022;59(4):2002732.
21. Pandey A, Shen C, Feng S, Man SM. Cell biology of inflammasome activation. Trends Cell Biol. 2021;31(11):924–39.
22. Wang L, Sharif H, Vora SM, Zheng Y, Wu H. Structures and functions of the inflammasome engine. J Allergy Clin Immunol. 2021;147(6):2021–9.
23. Rogiers O, Frising UC, Kucharíková S, Jabra-Rizk MA, van Loo G, Van Dijck P, et al. Candidalysin crucially contributes to Nlrp3 inflammasome activation by *Candida albicans* hyphae. mBio. 2019;10(1):e02221-18.
24. Sreejit G, Abdel-Latif A, Athmanathan B, Annabathula R, Dhyani A, NoothiSK, et al. Neutrophil-derived S100A8/A9 amplify granulopoiesis after myocardial infarction. Circulation. 2020;141(13):1080–94.
25. Sreejit G, Nooti SK, Jaggers RM, Athmanathan B, Ho Park K, Al-Sharea A, et al. Retention of the NLRP3 inflammasome-primed

neutrophils in the bone marrow is essential for myocardial infarction-induced granulopoiesis. Circulation. 2022;145(1):31–44.
26. Geng Y, Ma Q, Liu YN, Peng N, Yuan FF, Li XG, et al. Heatstroke induces liver injury via IL-1β and HMGB1-induced pyroptosis. J Hepatol. 2015;63(3):622–33.
27. Lian H, Fang X, Li Q, Liu S, Wei Q, Hua X, et al. NLRP3 inflammasome-mediated pyroptosis pathway contributes to the pathogenesis of *Candida albicans* keratitis. Front Med. 2022;9: 845129.
28. Zhang G, Wang J, Zhao Z, Xin T, Fan X, Shen Q, et al. Regulated necrosis, a proinflammatory cell death, potentially counteracts pathogenic infections. Cell Death Dis. 2022. https://doi.org/10.1038/s41419-022-05066-3.
29. Gong W, Shi Y, Ren J. Research progresses of molecular mechanism of pyroptosis and its related diseases. Immunobiology. 2020;225: 151884.
30. Zhang Z, Zhang Y, Lieberman J. Lighting a Fire: Can we harness pyroptosis to ignite anti-tumor immunity? Cancer Immunol Res. 2021;9(1):2–7.
31. Strowig T, Henao-Mejia J, Elinav E, Flavell R. Inflammasomes in health and disease. Nature. 2012;481:278–86.
32. Willingham SB, Allen IC, Bergstralh DT, et al. NLRP3 (NALP3, Cryopyrin) facilitates in vivo caspase-1 activation, necrosis, and HMGB1 release via inflammasome-dependent and - independent pathways. J Immunol. 2009;183:2008–15.
33. Yuan X, Wilhelmus KR. Toll-like receptors involved in the pathogenesis of experimental *Candida albicans* keratitis. Invest Ophthalmol Vis Sci. 2010;51(4):2094–100.
34. Kinoshita R, Sato H, Yamauchi A, Takahashi Y, Inoue Y, Sumardika IW, et al. exSSSRs (extracellular S100 soil sensor receptors)-Fc fusion proteins work as prominent decoys to S100A8/A9-induced lung tropic cancer metastasis. Int J Cancer Int J Cancer. 2019;144(12):3138–45.
35. Man SM, Karki R, Kanneganti TD. Molecular mechanisms and functions of pyroptosis, inflammatory caspases and inflammasomes in infectious diseases. Immunol Rev. 2017;277(1):61–75.
36. Wu Y, Zhang J, Yu S, Li Y, Zhu J, Zhang K, et al. Cell pyroptosis in health and inflammatory diseases. Cell Death Discov. 2022;8(1):191.
37. Austin A, Lietman T, Rose-Nussbaumer J. Update on the management of infectious keratitis. Ophthalmology. 2017;124(11):1678–89.
38. Brown L, Leck AK, Gichangi M, Burton MJ, Denning DW. The Global incidence and diagnosis of fungal keratitis. Lancet Infect Dis. 2021;21(3):e49–57.
39. Qiao GL, Ling J, Wong T, Yeung SN, Iovieno A. Candida keratitis: epidemiology, management, and clinical outcomes. Cornea. 2020;39(7):801–5.
40. Portnoy JM, Williams PB, Barnes CS. Innate immune responses to fungal allergens. Curr Allergy Asthma Rep. 2016;16(9):62.
41. Frosch M, Metze D, Foell D, Vogl T, Sorg C, Sunderkotter C, et al. Early activation of cutaneous vessels and epithelial cells is characteristic of acute systemic onset juvenile idiopathic arthritis. Exp Dermatol. 2005;14:259–65.
42. Henke MO, Renner A, Rubin BK, Gyves JI, Lorenz E, Koo JS. Up-regulation of S100A8 and S100A9 protein in bronchial epithelial cells by lipopolysaccharide. Exp Lung Res. 2006;32:331–47.
43. Yuan X, Hua X, Wilhelmus KR. The corneal expression of antimicrobial peptides during experimental fungal keratitis. Curr Eye Res. 2010;35(10):872–9.
44. Clohessy PA, Golden BE. Calprotectin-mediated zinc chelation as a biostatic mechanism in host defence. Scand J Immunol. 1995;42:551–6.
45. Sohnle PG, Hunter MJ, Hahn B, Chazin WJ. Zinc-reversible antimicrobial activity of recombinant calprotectin (migration inhibitory factor-related proteins 8 and 14). J Infect Dis. 2000;182:1272–5.
46. Clark HL, Jhingran A, Sun Y, Vareechon C, de Jesus CS, Skaar EP, et al. Zinc and manganese chelation by neutrophil S100A8/A9 (Calprotectin) limits extracellular aspergillus fumigatus hyphal growth and corneal infection. J Immunol. 2016;196(1):336–44.
47. Tartey S, Kanneganti TD. Differential role of the NLRP3 inflammasome in infection and tumorigenesis. Immunology. 2019;156(4):329–38.
48. Paik S, Kim JK, Silwal P, Sasakawa C, Jo EK. An update on the regulatory mechanisms of NLRP3 inflammasome activation. Cell Mol Immunol. 20211;8(5):1141–60.
49. Swanson KV, Deng M, Ting JP. The NLRP3 inflammasome: molecular activation and regulation to therapeutics. Nat Rev Immunol. 2019;19(8):477–89.
50. Liu Y, Beyer A, Aebersold R. On the dependency of cellular protein levels on mRNA abundance. Cell. 2016;165(3):535–50.
51. Buccitelli C, Selbach M. mRNAs, proteins and the emerging principles of gene expression control. Nat Rev Genet. 2020;21(10):630–44.
52. de Sousa AR, Penalva LO, Marcotte EM, Vogel C. Global signatures of protein and mRNA expression levels. Mol Biosyst. 2009;5(12):1512–26.
53. Kim S, Jacobs-Wagner C. Effects of mRNA degradation and site-specific transcriptional pausing on protein expression noise. Biophys J. 2018;114(7):1718–29.
54. Zong M, Bruton JD, Grundtman C, Yang H, Li JH, Alexanderson H. TLR4 as receptor for HMGB1 induced muscle dysfunction in myositis. Ann Rheum Dis. 2013;72(8):1390–9.
55. Laouedj M, Tardif MR, Gil L, Raquil MA, Lachhab A, Pelletier M. S100A9 induces differentiation of acute myeloid leukemia cells through TLR4. Blood. 2017;129(14):1980–90.
56. Martinon F, Burns K, Rg TJ. The inflammasome: a molecular platform triggering activation of inflammatory caspases and processing of proIL-beta. Mol Cell. 2002;10:417–26.
57. Kelley N, Jeltema D, Duan Y, He Y. The NLRP3 inflammasome: an overview of mechanisms of activation and regulation. Int J Mol Sci. 2019;20:3328.
58. Liu M, Li C, Zhao GQ, Lin J, Che CY, Xu Q, et al. Boxb mediate BALB/c mice corneal inflammation through a TLR4/MyD88-dependent signaling pathway in Aspergillus fumigatus keratitis. Int J Ophthalmol. 2018;11(4):548–52.
59. Yuan X, Mitchell BM, Wilhelmus KR. Gene profiling and signaling pathways of *Candida albicans* keratitis. Mol Vis. 2008;14:1792–8.
60. Ma L, Sun P, Zhang JC, Zhang Q, Yao SL. Proinflammatory effects of S100A8/A9 via TLR4 and RAGE signaling pathways in BV-2 microglial cells. Int J Mol Med. 2017;40(1):31–8.
61. Li K, Chen G, Luo H, Li J, Liu A, Yang C, et al. MRP8/14 mediates macrophage efferocytosis through RAGE and Gas6/MFG-E8, and induces polarization via TLR4-dependent pathway. J Cell Physiol. 2021;236(2):1375–90.
62. Kraakman MJ, Lee MK, Al-Sharea A, Dragoljevic D, Barrett TJ, Montenont E, et al. Neutrophil-derived S100 calcium-binding proteins A8/A9 promote reticulated thrombocytosis and atherogenesis in diabetes. J Clin Invest. 2017;127(6):2133–47.
63. Wellington M, Koselny K, Sutterwala FS, Krysan DJ. Candida albicans triggers NLRP3-mediated pyroptosis in macrophages. Eukaryot Cell. 2014;13:329–40.
64. Oliva K, Barker G, Rice GE, Bailey MJ, Lappas M. 2D-DIGE to identify proteins associated with gestational diabetes in omental adipose tissue. J Endocrinol. 2013;218(2):165–78.
65. Rubartelli A. DAMP-mediated activation of NLRP3-inflammasome in brain sterile inflammation: the fine line between healing and neurodegeneration. Front Immunol. 2014;5:99.
66. Ji Q, Wang L, Liu J, Wu Y, Lv H, Wen Y, et al. Aspergillus fumigatus-stimulated human corneal epithelial cells induce

pyroptosis of THP-1 macrophages by secreting TSLP. Inflammation. 2021;44(2):682–92.

Publisher's Note Springer Nature remains neutral with regard to jurisdictional claims in published maps and institutional affiliations.

Springer Nature or its licensor (e.g. a society or other partner) holds exclusive rights to this article under a publishing agreement with the author(s) or other rightsholder(s); author self-archiving of the accepted manuscript version of this article is solely governed by the terms of such publishing agreement and applicable law.